Water Adsorption on Activated Carbons: Study of Water Adsorption in Micro- and Mesopores

Juan Alcañiz-Monge,*,†,‡ Angel Linares-Solano,† and Brian Rand‡

Departamento de Química Inorgánica, Universidad de Alicante, Alicante E-03080, Spain, Department of Materials, University of Leeds, Leeds LS2 9JT, U.K.

Received: February 21, 2001; In Final Form: June 18, 2001

The mechanism of water adsorption is analyzed in a range of activated carbons differing widely in the relative proportions of narrow and wide micropores, mesopores, and macropores. They also display different degrees of surface functionality. By assuming that the adsorbed phase in micropores is "ice-like", it is shown that the whole micropore volume is filled with water at a P/P_0 of about 0.82, at which point capillary condensation may begin. However, surface complexes control the wetting of the mesopore walls by adsorbed water and can influence the condensation process. Condensation in macropores may also occur at P/P_0 values above 0.95. The extent of meso-/macropore filling depends on the surface complexes. The volume filling process is progressive and in micropores is consistent with the theory of volume filling. The adsorption process was analyzed by interpreting the nitrogen isotherms systematically measured on samples of different pore structure with progressively increasing amounts of preadsorbed water up to saturation.

Introduction

In many gas treatment processes involving activated carbons (ACs), water vapor is often present and can decrease their performance.[1−6] However, the mechanism of water adsorption in carbon materials is complex compared to that of conventional adsorptives (N_2, benzene, and CO_2).[7−15] Two main theories have been invoked to explain the phenomenon of water adsorption in carbon materials.

(1) Water adsorption occurs through a capillary condensation mechanism.[7,16−22]

(2) Water adsorption occurs according to the Dubinin−Serpinsky mechanisms involving clustering around primary adsorption centers.[8]

The first of these is based on the presence of adsorption hysteresis in the water adsorption isotherms, which is usually associated with the mechanism of capillary condensation.[7,16] Juhola[17,22] used the Kelvin equation to analyze water adsorption isotherms, suggesting they were suitable alternatives to N_2 adsorption for the assessment of pore size distributions. However, both the surface groups and the mineral matter are known to affect the water adsorption isotherm, and so, this method has not received widespread recognition.[23] The principal objection has been that the Kelvin equation has no physical basis when applied to water adsorption in micropores because the concepts of meniscus and surface tension lose their macroscopic sense in pores where there is space for only a few adsorbed layers (i.e., 5−7).[7]

The second mechanism, first postulated by Pierce and Smith[24] and further developed by Dubinin and Serpinsky,[8,16,25,26] is supported by numerous studies of microporous ACs, which demonstrate a strong influence of surface oxygen complexes on the water adsorption isotherm. In this mechanism, it is assumed that water adsorption occurs through the formation of clusters of chemisorbed water at active sites that are present on the carbon surface (surface groups), followed by the growth and coalescence of these clusters.[8,26] Thus, the surface density and character of these groups controls the relative pressures at which water adsorption starts. Recently, computer simulation studies,[27,28] have also indicated that the adsorption of water occurs via the formation of three-dimensional clusters on oxygenated sites, again emphasizing the predominant role that the surface groups have on the water adsorption mechanism.

In situ studies of water adsorption using X-ray diffraction and small-angle X-ray scattering have shown that the water molecules are confined in carbon micropores.[29−33] Nevertheless, most studies on the adsorption of water by microporous carbons consider that the surface groups play the main role.[7−15,34−42] The focus of many of these studies has been to analyze the role of surface groups (amount and type) by subjecting the ACs to controlled oxidative treatments (in many case very strong, e.g., with hot nitric acid). These treatments can develop a surface chemistry often very different from that which normally prevails on the surface of commercial ACs, leading to higher concentrations of species with different functionalities. Thus, in these studies, the influence of pore size on the mechanism of water adsortion is masked by the higher amount of surface groups. As a consequence, it can be stated that the analysis of water isotherms on porous carbon materials is not sufficiently well understood. In particular, there has been little systematic study of the influence of pore size on the mechanism of water adsorption, and the adsorption of water in the mesopores of AC has scarcely been studied at all. It is noteworthy in this respect that Kaneko recently suggested that water does not adsorb in the mesopores.[43,44]

In previous studies, we have investigated the water adsorption in AC fibers (ACFs), which are mainly microporous solids with a well-defined porosity and a relatively low surface concentration of oxygenated groups.[45] By reducing the influence of the surface complexes, we were able to show that water adsorption in micropores depends on the micropore size, taking place

* Corresponding author. E-mail: Jalcaniz@ua.es.
† Universidad Alicante.
‡ Leeds University.

10.1021/jp010674b CCC: $20.00
Published on Web 07/31/2001

TABLE 1: Characteristics of the Activated Carbons (AC) Used

sample	supplier	precursor	activation method
CFC20	−	fiber from petroleum pitch	CO_2
CFS79	−	fiber from petroleum pitch	steam
KUA1	−	anthracite	Chemical:KOH
A	−	phenolic resin	Carbonized/N_2
SCII (ref. GR 31124A)[a]	Chemviron	coconut	−
BH45	−	almond shell	CO_2
Darko (G-60)	Aldrich	−	−
BPL (ref. GR 31124E)[a]	Chemviron	bituminous coal	−
Westvaco (SA-30)	Westvaco	Wood	Chemical:HPO_3

[a] Specially prepared samples.

gradually according to the pore size. First, the narrow micropores and then the wider ones are filled. It was concluded that the adsorbed water in the microporosity is in a solid, ice-like phase, with a density around 0.92 g cm^{-3}. This paper presents the results of an extension of this study to ACs obtained from different precursors, now covering a wide range of pore volumes with materials selected with different contributions from mesoporosity and microporosity to enable the influence of the mesopores on the water adsorption isotherm to be more clearly observed.

2. Experimental Section

Water adsorption was studied on a series of commercial activated carbons (BPL, SCII, Darko, and Westvaco) and samples prepared in the laboratory (CFC20, CFS79, KUA1, A, and BH45). Table 1 summarizes the raw materials and activation methods in each case. Activated carbon fibers were prepared by the physical activation of a commercial petroleum pitch-based carbon fiber (Kureka) in CO_2 up to a 20% burnoff (CFC20) and in steam up to a 79% burnoff (CFS79);[45,46] KUA1 was prepared by chemical activation of a Spanish anthracite[47] and BH45 by physical activation of a ligno-cellulose-based carbon,[48] while sample A is a phenol−formaldehyde polymer resin char.[49]

Porous texture analysis of these samples was carried out by gas adsorption (N_2 and CO_2 at 77 and 273 K respectively, using the Quantachrome Autosorb 6) and by mercury porosimetry (Carlo Erba 2000). The samples were outgassed at 623 K under vacuum, at 10^{-6} Torr. The Dubinin−Radushkevich (DR) equation[7,50] was used to calculate the micropore volume. The different pore volumes used in our discussion were calculated as follows:[51] From the CO_2 DR plots (relative pressures < 0.015), the volume of narrow micropores (pore size < 0.7 nm) was calculated (V_C) . The total micropore volume, V_{mic} (pore size < 2 nm), was calculated from the N_2 DR plot (relative pressures < 0.14) and includes the volume of the narrow micropores and the supermicropores. The mesopore volume, V_{mes}, (2 nm < pore size < 50 nm) was estimated by combining data from the N_2 isotherm (i.e., amount adsorbed between $P/P_0 = 0.3-0.7$), which gave the volume in pores up to 3 nm radius, with data from mercury porosimetry, which gave the volume in pores from 3 to 25 nm in radius. The macropore volume, V_{mac} (50 nm < pore size), was obtained from mercury porosimetry.

Water adsorption measurements were carried out at 298 K in an automatic volumetric gas adsorption instrument (Belsorp 18). It should be noted that there are difficulties in accurately measuring pressures above 0.98 in more conventional gas adsorption equipment, due both to water condensation on the wall of the instrument and to the long time taken to come to equilibrium. This instrument is designed to avoid the condensation of water vapor on the walls of the apparatus and can be operated for long times (40−80 h). Experimental data were corrected for adsorption on the inner wall of the apparatus. A more detailed description of the system is given elsewhere.[52] Additionally, a blank run on all the bulbs showed that water adsortion on the inner surface of the glass was negligible. Samples were degassed at 623 K under high vacuum (10^{-6} Torr). The mechanism of water adsorption was further analyzed by remeasuring the N_2 adsorption on ACs with a certain amount of water preadsorbed. To do this, the water adsorption in a sample was stopped at a certain relative pressure; the bulb was closed and then the sample analyzed by N_2 adsorption at 77 K. The same procedure was applied to the analysis of the transition between meso- and macroporosity with highly hydrated samples were also analyzed by mercury porosimetry. These highly hidrated samples were immersed in pure distilled water, and after introduced into a desiccator for a period of time.

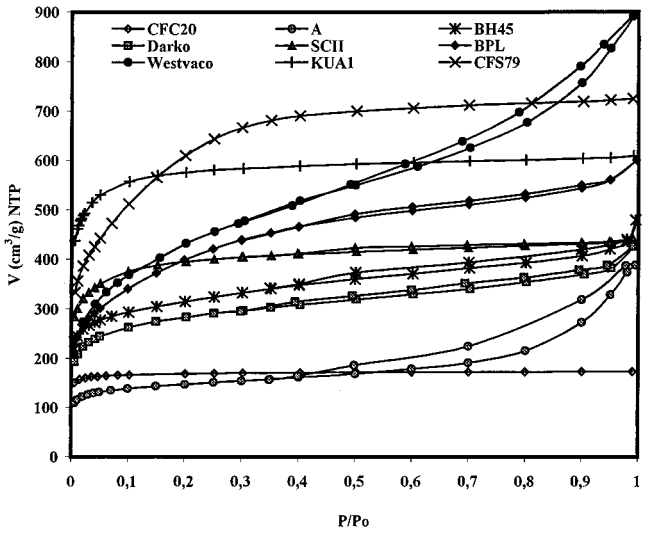

Figure 1. N_2 isotherms of the activated carbons.

3. Results and Discussion

3.1. Textural Characterization of Activated Carbons. Figure 1 shows the nitrogen isotherms of the ACs. All samples are microporous and show considerable uptake of nitrogen at low relative pressures (<0.2).[53] However, the nitrogen uptake at relative pressures (P/P_o) > 0.2 in some samples shows that these are also mesoporous. These isotherms demonstrate that the samples cover a wide range of pore volume, with varying capacity of N_2 adsorption. They can be divided into two groups, those which are essentially microporous without any mesoporosity which show true type I isotherms [CFC20, CFS79, SCII, and KUA1] and those which display additional meso- and macroporosity. In the latter group, the volume ratios of each pore type vary significantly.

Figure 2 shows the cumulative pore volume distribution obtained from mercury porosimetry. The samples having no macro- and mesoporosity, CFC20, CFS79, and KUA1, are not represented. The results show that SCII has a very small macropore volume, although this is not clearly evident in the N_2 isotherm. Samples BH45 and Darko have similar, low mesopore volumes, consistent with the similar shapes of their nitrogen isotherms, but they display quite different macropore volumes. The higher macropore volume of Darko can be partly

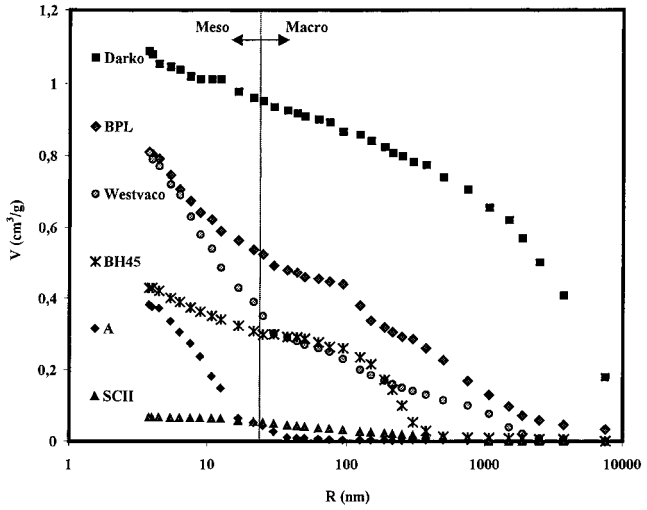

Figure 2. Cumulative pore volume distributions of the carbons, from mercury porosimetry.

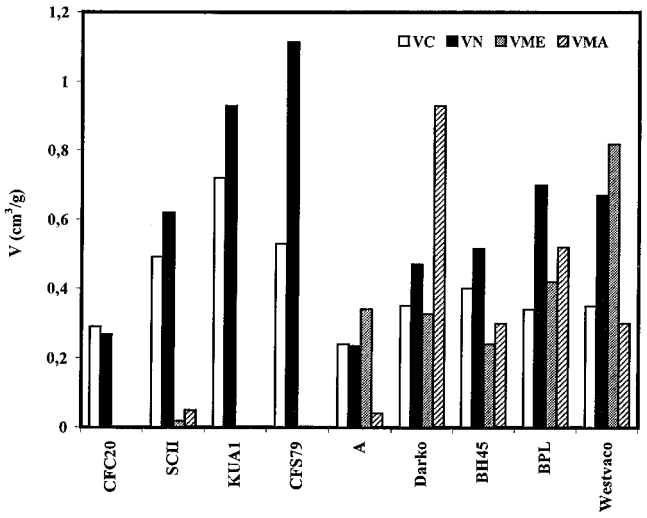

Figure 3. Histograms showing the different pore volumes of the various ACs: narrow microporosity (V_C), all microporosity (V_{mic}), mesoporosity (V_{mes}), and macroporosity (V_{mac}).

related to the interparticle space. Sample A contains only mesoporosity but at an appreciable volume. Finally, Westvaco and BPL samples have high mesopore volumes as well as a considerable macropore volume.

To analyze the pore volume distribution more completely, Figure 3 shows the volumes of pores in different size ranges. The comparison of both V_C (narrow micropore, <0.7 nm) and V_{mic} (micropore, <2 nm) gives an idea the size of the micropores, while from V_{mic}, V_{mes}, and V_{mac}, we deduce the total pore size distribution. From Figure 3, it can be seen that $V_{mic} = V_C$ for CFC20, showing that all the micropores are narrow in this sample. In other samples, there is a wide micropore size distribution, the size and volume increasing in the order SCII < KUA1 < CFS79 (as deduced from the comparison of the V_{mic} and V_C values and the opening of the knee of the nitrogen isotherm (Figure 1)). Sample A[49] contains both micropores and mesopores, the mesopore volume being the higher of the two. However, the similarity between V_{mic} and V_C (Figure 3) and the sharp knee of the isotherm (Figure 1) indicates that the micropores are quite narrow (around 0.7 nm) in this carbon. Samples Darko and BH45 are quite similar, with a mesopore volume comparable to that of sample A, but they have slightly wider micropores and a higher micropore volume. Their

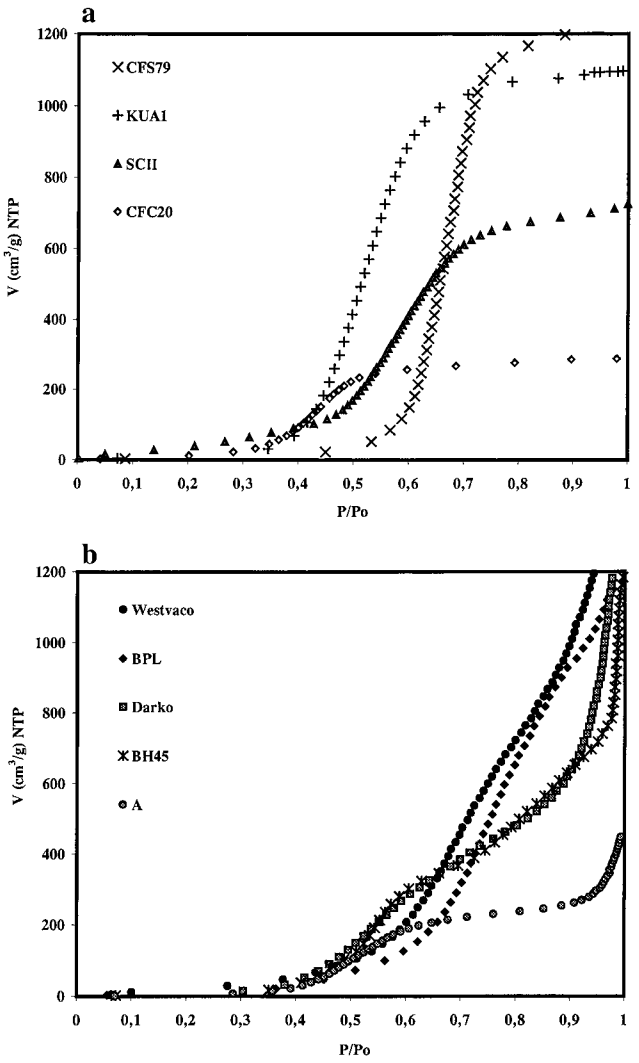

Figure 4. Water adsorption isotherms on the essentially microporous ACs (a) and on the ACs with different contributions of micro, meso, and macroporosity in (b).

isotherm shapes are similar to each other (Figure 1) and they have a similar relationship between the different volumes V_C, V_{mic}, and V_{mes} (Figure 3). Thus, these samples differ only in their macroporosity. Finally, BPL and Westvaco also have micropore volumes and size distributions similar to each other. They also have the widest micropore size distributions of all the samples and the highest mesopore volumes. The Westvaco samples, in fact, show the highest mesopore volumes of all (Figures 1 and 2). Both of these last two samples display an appreciable macropore volume.

The porous texture of the samples studied show significant differences in pore size distributions and pore volume and thus are very suitable for an analysis of water adsorption in the different ranges of pore size.

3.2. Water Adsorption Isotherms. Figure 4a shows water adsorption isotherms on those ACs which are entirely or substantially microporous, while those for the ACs with significant contributions of micro-, meso-, and macroporosity are shown in Figure 4b (in which for comparison purposes, the full isotherms, near saturation, are not shown). The isotherms in Figure 4a are type V, characteristic of water adsorption in microporous ACs.[53] Water adsorption is largely confined to the P/P_0 range 0.3−0.8. The precise isotherm shape is a function of the micropore size because the steep part of the adsorption isotherm and the "knee" shift to lower relative pressures as the

TABLE 2: Pore Volumes ($cm^3\ g^{-1}$) Deduced from N_2 Adsorption and Mercury Porosimetry Compared with Values from H_2O Adsorption

	V_{mic}	V_{H_2O} (0−0.82)	V_{mac}	V_{mes}	V_{H_2O} (0.82−1)
CFC20	0.29	0.27	–	–	–
SCII	0.62	0.61	0.05	0.02	–
KUA1	0.93	0.94	–	–	–
CFS79	1.14	1.10	–	–	–
A	0.24	0.21	0.04	0.34	0.19
Darko	0.47	0.44	0.93	0.33	0.82
BH45	0.52	0.46	0.30	0.24	0.59
BPL	0.70	0.67	0.52	0.42	0.81
Westvaco	0.67	0.67	0.30	0.82	0.82

micropore size (based in Figure 3) decreases, i.e., CFC20 < A< KUA1 = SCII < CFS79. This is in agreement with the results obtained previously for AC fibers.[45] Interestingly, the water isotherm of sample A in Figure 4b displays two well-defined ranges of water adsorption, the initial part due to water adsorption in micropores and an additional region of adsorption at high relative pressures ($P/P_0 > 0.9$) which does not show up in the microporous samples (Figure 4a) and must be related to adsorption in the mesopores.

The water isotherms of those ACs with significant mesoporosity (Figure 4b) are more complicated, resembling a combination of type III and V isotherms.[53] Those samples with similar micropore size distributions (BH45-Darko and BPL-Westvaco) have similar water isotherms in the range of relative pressures < 0.8, while at high relative pressures ($P/P_0 > 0.8$), they behave in accord with their different meso- and macropore size distributions. Thus, according to the pore size distribution and the contribution of the different pore volumes, the water isotherm can be type V, with essentially microporous ACs, or type III for ACs, with a wider pore size distribution and similar micro- and mesopore volumes. Thus, the water isotherm on sample A displays a clear distinction between the two regions of pore size, due to it having a well-defined transition between both kinds of porosity. As has been commented previously,[45] as the micropore size increases, water adsorption shifts to higher relative pressures. Therefore, when a clear transition does not exist between the micro- and mesoporosity, both the final filling of the micropores and the start of capillary condensation in mesopores can take place in the same range of relative pressures, the overlapping processes giving a single curve. All of these points are reflected in Figure 4b. So it can be seen clearly that two regions of water adsorption take place in the samples BH45-Darko, whereas on BPL-Westvaco, the distinction is not so evident. There is a clear correlation with the pore size distributions of the samples (Figure 3).

It seems clear from this and the previous study[45] that water adsorption up to P/P_0 of about 0.8 is due to micropore filling and at higher P/P_0 due to the filling of the mesopores and/or macropores. From a visual analysis of all the isotherms in this and the previous work, a value of $P/P_0 = 0.82$ is a good approximation for the relative pressure at which the micropore volume is filled with adsorbed water for all samples. This approach was used to estimate to the micropore volume. A similar approximation had been made by Lodewyckx and Vansant.[54]

Table 2 compares the micro and combined meso- and macropore volumes of the samples, estimated from water adsorption, with those from N_2 and mercury porosimetry, already discussed. The meso-macropore volumes were calculated from the difference between the amounts of water adsorbed at saturation and at $P/P_0 = 0.82$. According to the previous work,

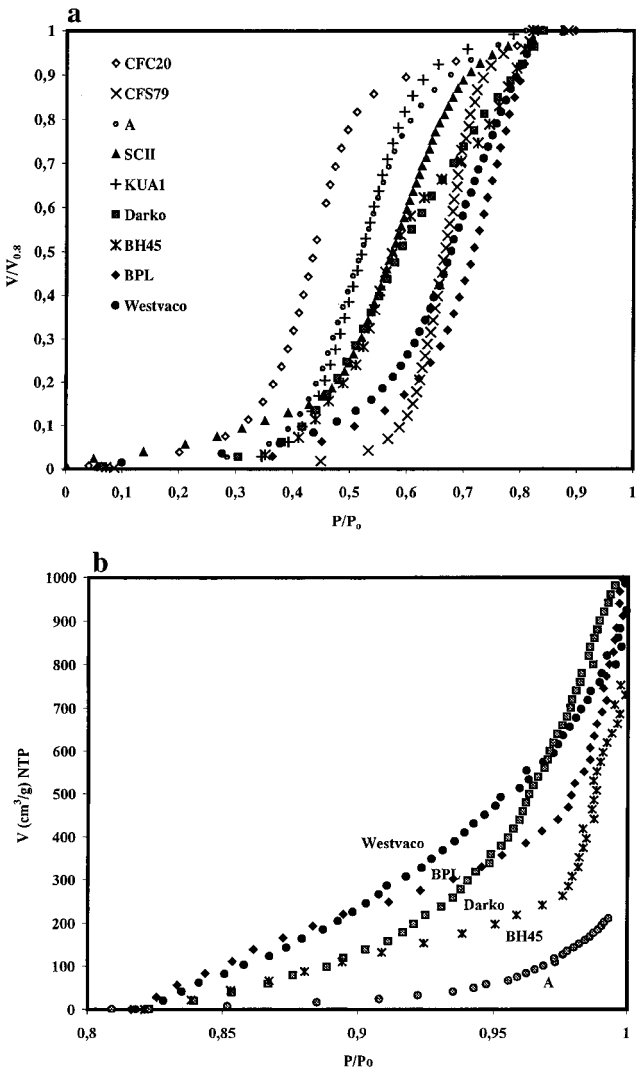

Figure 5. Water adsorption isotherms (a) normalized to the value at $P/P_0 = 0.82$ ($N/N_{0.82}$); (b) water adsorption isotherms from $P/P_0 = 0.82$.

we have used the value of 0.92 g cm^{-3} as the density of water adsorbed in carbon micropores.[45] However, water adsorbed in mesopores is likely to have a density closer to that of liquid water, and so, the liquid density value has been used to calculate the volume of pore space filled with adsorbed water at $P/P_0 > 0.82$. Table 2 shows that the micropore volumes obtained from the amount of water adsorbed at $P/P_0 = 0.82$ agrees quite well with the corresponding N_2-derived micropore volumes. The agreement is especially good for the samples with little or no mesoporosity but is remarkable for the others, considering that adsorption in the two types of pores overlaps. This result suggests that the approach is sound and confirms again that water adsorbs in the whole micropore volume. Considering the variety of ACs employed in this study, it seems to be a generalized fact that the water adsorbed in micropores is present in a solidlike structure (density 0.92 g cm^{-3}). This confirms the use of the density of ice to calculate the micropore volume in ACs.[45]

To analyze more completely the adsorption of water in the micropores, all the samples represented in Figure 4 have been normalized with reference to the value that their presents at $P/P_0 = 0.82$. Figure 5a shows such normalized plots. From it, we can observe that the isotherm shape is very dependent upon the micropore size distribution of the AC (Figure 3), and it

further emphasizes the influence exercised by the micropore size in determining the water isotherm shape.[34,45,55−57] This is not to deny the importance of surface oxygen complexes, but the water adsorption on these complexes takes place at relative pressures below the steep rise in the isotherm and represents only a small proportion of the total water adsorbed in the micropores,[13,54] determining merely the position of the onset of adsorption. A curious general relationship seems to exist (except CFS79 sample) between the slope of the isotherm lineal tract (Figure 5a) and the micropore size distribution. Thus, sample CFC20 has both a high slope of the isotherm lineal tract and a narrow micropore size distribution, whereas sample Westvaco has a minor slope and a broad micropore size distribution (see Figures 3 and 5a). It is also interesting that the isotherms for samples Darko and BH45 (Figure 5a) exhibit two inflections, showing that water adsorption also seems to be quite sensitive to the detail of the micropore size distribution.

Table 2 also compares the values of $V_{mes} + V_{mac}$ determined from N_2 adsorption with the volume occupied by water adsorbed in the region of P/P_0 0.82−1, assuming that the latter is in the form of a liquid and hence its density is 1 g cm^{-3}. It appears that the amount of water adsorbed in this range of pore size depends on sample type. Thus, samples BH45 and BPL display similar volumes, indicating that water adsorbs in the whole pore volume, whereas for samples Westvaco and A, this is not always the case. From the values obtained for Darko, BH45, and BPL, it is clear that the water adsorbs in the macropores, since the pore volume obtained from water adsorption is twice as that of the mesopore volume. This is greatly different from that of conventional adsorptives (N_2 and C_6H_6), which do not show adsorption in macropores or in large mesopores.[7] This difference is due to the high surface tension of water in comparison with the other liquid adsorptives. Juhola[22] suggested that this property of water, together with its small molecule diameter and the fact that it is not strongly adsorbed on activated carbon, makes water a suitable adsorptive for determining the pore size distribution of carbon, allowing it to cover a wider range of pore diameters (2−400 nm) than those of other adsorptives. [22]

To more easily compare the isotherms in the range of relative pressure 0.82−1, because there are samples for which the pore volume is not totally filled by the water, they have been normalized using the value at $P/P_0 = 0.82$ as the origin (Figure 5 b). In general, up to relative pressures of about 0.9−0.95, the order of the isotherms and of the amounts of water adsorbed follows the same trend as that of the mesopore volume (Figure 3). At relative pressures higher than 0.95, there is a sharp increase in the water uptake for BPL and BH45 and also for Darko but with not such a clear discontinuity as that in the latter case. This seems to be indicative of the start of condensation in macropores. The amounts adsorbed at this P/P_0 (0.95) are coincident with the mesopore volumes. The concept of capillary condensation would require that the mesopores are filled prior to the macropores, and this is what is observed.

A study of the transition in the filling of both types of pore is interesting. For example, BH45 and BPL show a clear transition; for Darko it is more smooth, but for Westvaco and A, it is not evident. For sample A, this is because this material displays very little macroporosity. For BH45 and BPL, the effect is due to the fact that the pore size distribution in the meso/macropore range is bimodal (Figure 2). Samples Darko and Westvaco have a continuous pore size distribution in this range, which explains why no discontinuity exists in the water isotherm of the former at these high relative pressures. However, the macropore volume of sample Darko is not completely filled with adorbed water, as shown in Table 2. This is undoubtedly because the macropore volume assessed by mercury penetration includes a significant amount of interparticle pore space in this case. The Westvaco sample should not be expected to show any inflection in the water isotherm at $P/P_0 > 0.95$ because it also has a continuous distribution of pore size. However, it would appear that water adsorption in the mesopores of Westvaco and also of sample A occurs at a P/P_0 higher than those of the other samples, and according to Table 2, their meso/macropore volume is not completely filled. A similar result was obtained with mesoporous carbon aerogels by Hanzawa and Kaneko,[43,44] who reported that water does not adsorb in carbon mesopores. However, the above results show that in certain cases, it does. The different behavior of the other two samples is analyzed in the next section.

3.3. Characterization of Porous Texture of Partially Hydrated Samples. To confirm that the mesopore volume of sample A and the meso- and macropore volumes of the Westvaco sample are not completely filled with adsorbed water, the procedure used previously[45] to elucidate the mechanism of water adsorption in micropores was adopted, in which samples with water preadsorbed to saturation were further characterized by N_2 adsorption. In this procedure, only the Westvaco and sample A showed any N_2 adsorption, which demonstrates that there is available surface area in these two samples saturated with water and that the pore space of the other samples is completely filled. Hence, it is clear that there is a meso- and/or macropore volume in which water is not adsorbed in these samples.

To study in more detail the mechanism whereby water is adsorbed into the pore structure, a similar procedure was used but with different amounts of preadsorbed water. The water adsorption in a sample was stopped at a certain level of filling. As an example, Figure 6 shows the fractional filling of water used for samples Westvaco and A (Figure 6a,b) and the corresponding N_2 isotherms for each (Figure 6 c and d). For a better analysis, Table 3 shows the fractional filling of the different pore volumes with water at each relative pressure of water at which the isotherm was halted. In this procedure, the unfilled micropore volume was estimated at $P/P_0 = 0.3$ on the nitrogen isotherm of the partially saturated sample (which is very close to the micropore volume) and the unfilled mesopore volume from the difference between this value and the amount adsorbed at $P/P_0 = 1$. While the estimate of the unfilled micropore volume should be quite accurate, the nitrogen isotherm on these partially saturated materials cannot be used to assess any changes in the macropore volume. As observed, there is a progressive reduction in N_2 adsorption capacity with the increase in amount of water preadsorbed, which is similar for all the samples studied. The appreciable N_2 adsorption observed in the saturated Westvaco and A samples occurs by capillary condensation in the mesopores and multilayer adsorption on the surfaces of macropores.

The above comparison of nitrogen isotherms with the corresponding point on the water isotherm shows that the water adsorbed at low P/P_0 produces only a decrease in the micropore volume equivalent to the fractional filling with water (Table 3). Thus, there is a progressive reduction in micropore volume without any change in the mesoporosity until a P/P_0 around 0.82, where the micropore volume is nearly filled. This result confirms the approximation made above that in this range of relative pressure, water adsorbs only in micropores. From different experiments, Hanzawa and Kaneko[43,44] made a similar conclusion, that the adsorption of water vapor on AC in the

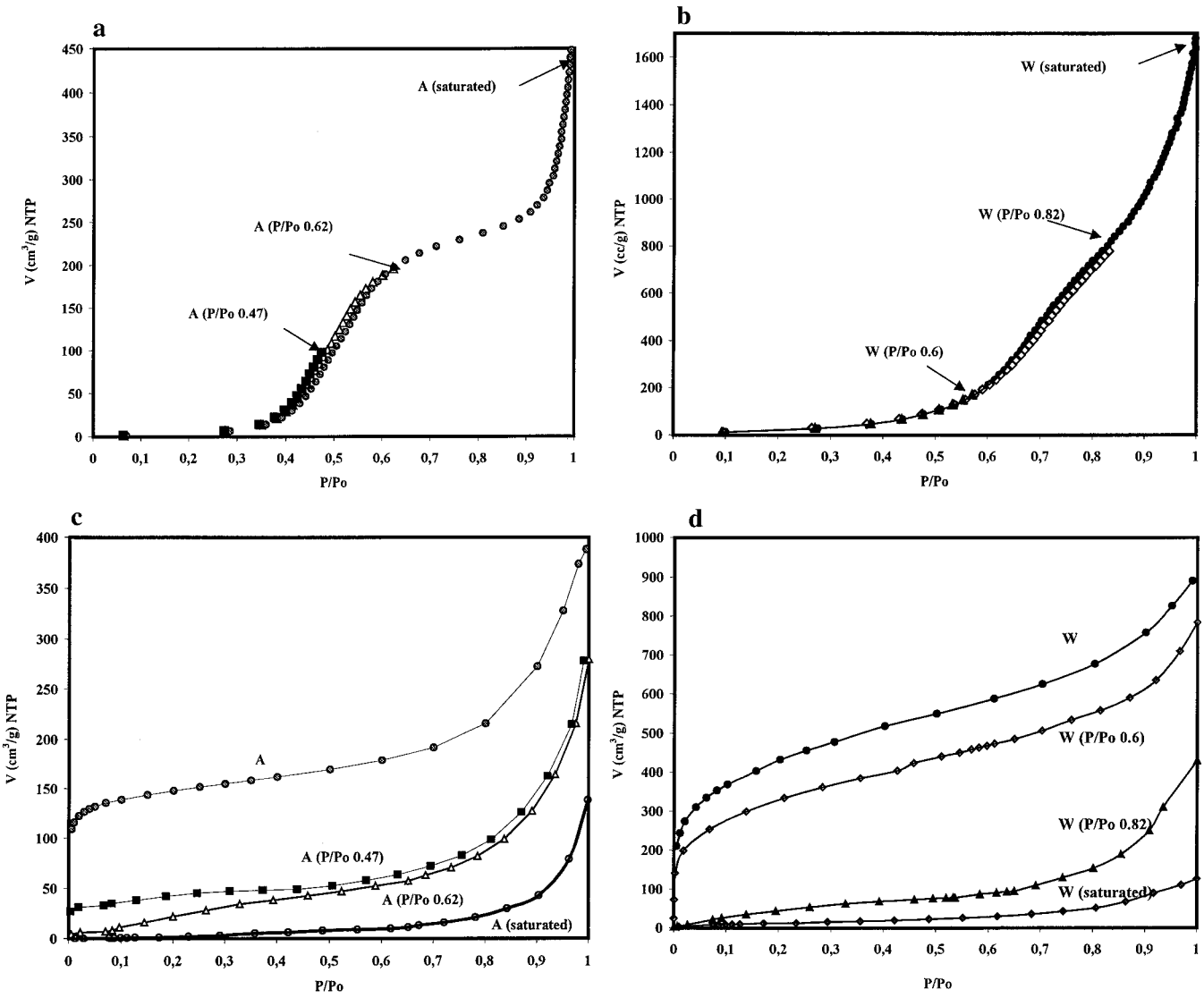

Figure 6. Water isotherms on carbons Westvaco (a) and A (b), showing the different degrees of water uptake at which the adsorption was arrested prior to N_2 adsorption characterization; the corresponding N_2 isotherms of Westvaco (c) and A (d**)** at the different degrees of water uptake.

TABLE 3: Pore Volume Reduction (%) Due to Different Amounts of Preadsorbed Water, as Deduced from N_2 Isotherms

sample	P/P_0 of preadsorbed water	V_{mic} (%) precursor	V_{mes}
Westvaco	0.60	22	1
Westvaco	0.82	90	9
Westvaco	1	100	73
A	0.47	70	0
	0.62		
	1		
A		80	0
A		100	65
BPL	0.79	78	0
BPL	1	1	100
BH45	1	100	100
darko	1	100	100

middle range of P/P_0 is not ascribable to a capillary condensation mechanism. It also agrees with the conclusions from a previous study of water adsorption in the micropores of AC fibers[45] that narrower micropore are filled first and water is ultimately adsorbed in the whole range of microporosity. The next section will analyze how water adsorbs in the meso- and macropore size range.

To investigate more fully the transition from adsorption in mesopores to that in macropores, the characterization of partially hydrated samples was continued. However, in this case, the analysis of the unfilled pore volume and size distribution must be carried out with mercury porosimetry. In this case, the amount of water adsorbed was expressed as a weight percentage of the AC sample (see Experimental Section). The BPL sample was chosen because it displays a clear transition around $P/P_0 = 0.98$ in the water isotherm (Figure 5b). Figure 7 shows the cumulative pore volume distribution from mercury porosimetry of this sample degassed and with 130 and 150 wt % of adsorbed water (corresponding to amounts adsorbed at $P/P_0 > 0.995$). The adsorbed water progressively decreases both the meso- and macropore volumes accessible to mercury. In the sample with 150 wt % adsorbed, there is no evidence of mesoporosity and the macropore volume is reduced. Hence, from these experiments, it is evident that water adsorb first in mesopores and then in the macropores. Similar results had been obtained by Lentz and Zhou,[58] who concluded that water adsorbs first in the small pores.

3.4. Study of Mechanism of Water Adsorption on AC. The results obtained in this work will now be analyzed in the context of the island cluster and capillary condensation approaches to water adsorption discussed in the Introduction. The results and discussion presented above show that it is reasonable to consider

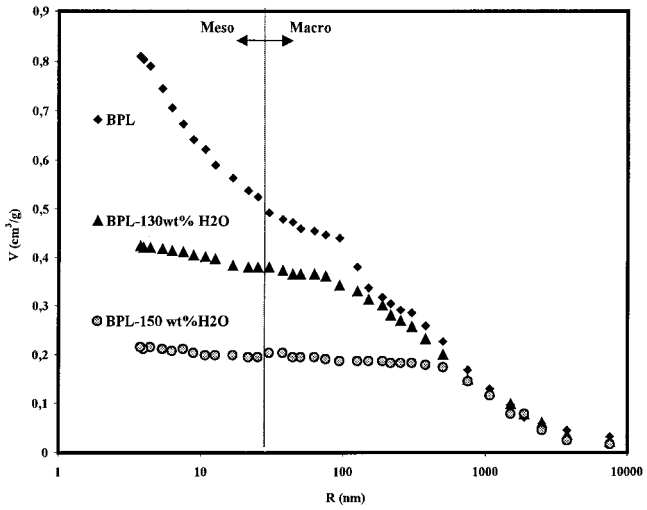

Figure 7. Cumulative pore volume distributions from mercury porosimetry for sample BPL degassed and with 130 and 150 wt % of preadsorbed water.

that water adsorbs principally in the micropores up to about $P/P_0 = 0.8$, at which point filling of the mesopores begins and then, at P/P_0 close to saturation, volume filling of the macropores takes place (Figure 5b). Thus, volume filling of the pores of ACs occurs during water adsorption but via different mechanisms according to the pore size. Considering the two approaches, it is reasonable to conclude that, in principle, both mechanisms are valid but they principally apply to different ranges of relative pressures. Thus, water adsorption at low P/P_0 is influenced by the island-cluster mechanism, the micropores are filled with water in an "ice-like" state at P/P_0 of about 0.82, and at $P/P_0 > 0.8$, there is capillary condensation.

In previous work[45] with AC fibers, it was suggested that after the initial clustering process water fills the micropores according to the Polanyi−Dubinin potential theory, or the theory of volume filling of micropores (TVFM).[50,59] In this work, we find the same trend in a series of ACs typical of those used in commercial applications (Figure 5a) for the isotherm shape on the range of P/P_0 0.3−0.8 depends on the micropore size distribution, in accord with the TVFM theory. This is also in agreement with the conclusion of other researchers that water adsorption on microporous AC with low oxygen contents can be described by the DA approach.[54,60] The influence-exercised surface groups is manifested at low relative pressures (<0.3), but more importantly, they can impeded water adsorption in the micropores (by pore blocking) if degassing of the samples is not carried out correctly.

Figure 8a shows the water isotherm on sample CFC20 obtained at different temperatures, the water adsorption shifting to higher pressures as the adsorption temperature increases. According to the TVFM[59] the characteristic curve should be temperature-invariant; i.e., the data at different temperatures should coincide on a unique curve name the characteristic curve. Figure 8b shows the characteristic curves plotted in the DR coordinates for the narrow micropore material, CFC20, and the wide micropore sample CFS79. The density of solid ice has been used to calculate the filled micropore volume at all temperatures. Both show temperature-invariant curves, supporting the concept that the influence of the micropore size on the water adsorption accords with the potential theory.

From these results, the isosteric heats of adsorption was also estimated, using the Clausius−Clapeyron equation, $q_{st} = -R[(\partial \ln p)/\partial(1/T)]_n$, and found to be round 44−48 kJ mol^{-1},

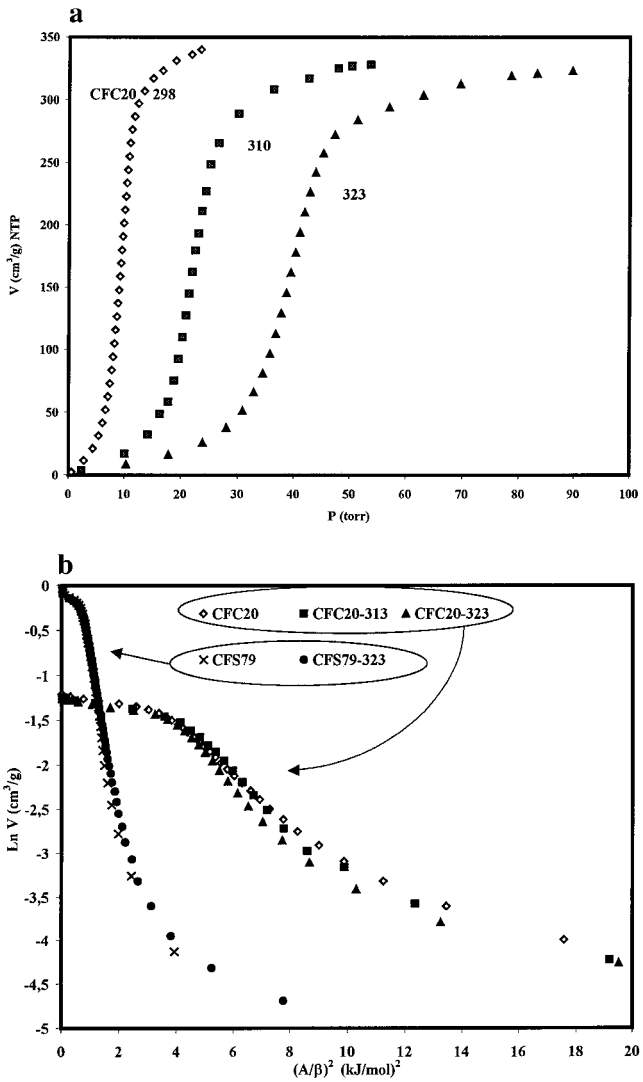

Figure 8. Water isotherms on sample CFC20 measured at different temperatures (298, 313, and 323 K) (a); DR characteristic curves obtained from the water isotherms at 298 and 323 K on samples CFC20 and CFS79 (b).

in agreement with other measurements[16,25,34,35,61,62] and very close to the normal enthalpy of water condensation (43.6 kJ mol^{-1}). It is also interesting that the density of water adsorbed in the micropores can be assumed not to change significantly in the range of temperature studied (298−323 K). Water molecules probably adsorb initially on the pore walls, possible associated with oxygen complexes which might exist, and then further adsorption of water molecules occurs at these sites promoted by hydrogen bonding. Finally, volume filling takes place according to the TVFM mechanism. This behavior is contrary to that of nonpolar adsorptives, where the interaction between walls and molecules is stronger than that between the molecules themselves. As a consequence of this mechanism, this analysis of the pore size distribution by the Kelvin method, in the range of P/P_0 0.3−0.8, seems not to be applicable. This is similar to the interpretation of isotherms for nonpolar adsorptives. A similar conclusion about the inapplicability of the Kelvin equation to analysis of water adsorption has been proposed by Kaneko et al.[44] However, their interpretation was made according to a new model of adsorption, the "cluster-mediated" water adsorption.[44,63] With this model, the experimental fact of the disappearance of the clear adsorption hysteresis in the case of water adsorption in narrow micropores

can be explained. However, our interpretation of water adsorption can also explain this behavior.

Water adsorption in the meso- and macropore range of P/P_0 0.8−1 should be mainly according to the capillary condensation mechanism, so in principle, it would seem to be correct to use the Kelvin equation to describe this adsorption mechanism.[7] This equation, with correction for the contact angle θ between liquid phase and pore wall, is

$$\ln\left(\frac{P_0}{P}\right) = \frac{2\sigma V m \cos\theta}{RTr_k}$$

where σ and V_m are, respectively, the surface tension and the liquid molar volume of bulk water at temperature T, R is the gas constant, and r_k is the core pore radius. For the case of water at 298 K, the liquid molar volume is $V_m = 18$ cm^3 mol^{-1}, and the surface tension is around $\sigma = 72$ mN m^{-1}. The most critical parameter is the contact angle, which for these carbon systems has a great uncertainty because liquid water does not wet the micropore wall due to the hydrophobicity of carbon. For example, depending upon the type of carbon, it can take different values; on pure graphite θ is 86°, on graphon 82°, and on pyrolytic carbon 72° at 298 K.[64] However, the presence of polar compounds on the surface of carbon can reduce the contact angle. As a consequence, the polarity and contact angle will vary according to the surface chemistry. This is in contrast to N_2 or benzene adsorptives which completely wet carbon (cos $\theta = 1$) and are not influenced by the presence of surface polarity. Hence, due to this strong dependence of θ on the polar nature of carbons, the Kelvin equation cannot be used satisfactorily for the analysis of pore size distribution from water adsorption isotherms. On the another hand, this helps to explain the different behavior that is shown by the samples studied here. Thus, sample A displayed water adsorption in the mesopores at a higher relative pressures than the other samples as a consequence of the poor wetting of water on this material. This is in agreement with the fact that this sample has not been exposed during its preparation to oxidative activation procedures, so it is reasonable to think that its surface should be less polar than the activated samples. The absence of water adsorption in the mesopores of carbon aerogels[44,45] may also be due to a high water contact angle on these solids, but it may also be because the experimental study attained a relative pressure of only 0.85, and according to our results, this is the value at which filling of the mesopores by adsorbed water begins.

Following the above considerations, water adsorption in the Darko sample after heat treatment at 1173 K was carried out and is compared with the original in Figure 9. It should be noted that while the heat treatment of Darko caused a weight loss of 9 wt %, fundamentally due to the decomposition of surface oxygenated groups, its micropore and mesopore volumes scarcely changed. Heat treatment is observed to shift the start of the water isotherm to higher relative pressures, around 0.8, in which region both isotherms overlap. This shift is most likely due to the reduced amount of oxygenated groups (assessed from TPD experiments, from 823 to 159 μmol/g) which influence the start of the water isotherms, but not the filling of the total micropore volume, and is entirely in accord with the proposed relative contributions of surface groups and micropore filling to the adsorption isotherm. However, these surface groups not only influence the P/P_0 at the start of water adsorption but also have an important on the adsorption in meso- and macropores and on the degree of filling of the mesoporosity, as deduced from the comparison between both isotherms in the range of

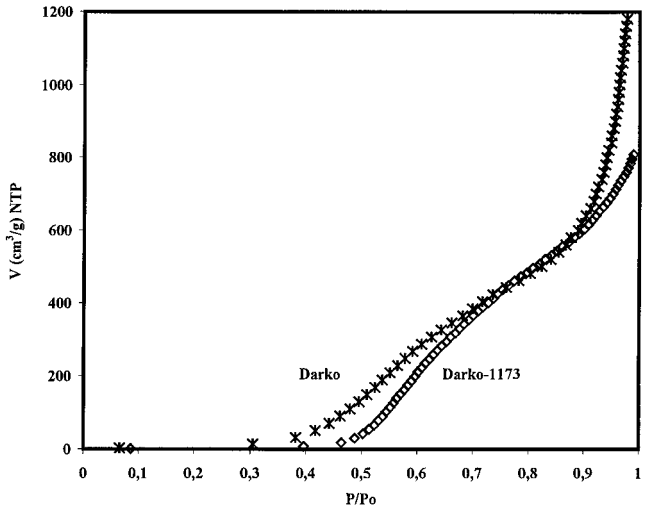

Figure 9. Water adsorption on Darko before and after heat treatment at 1173 K.

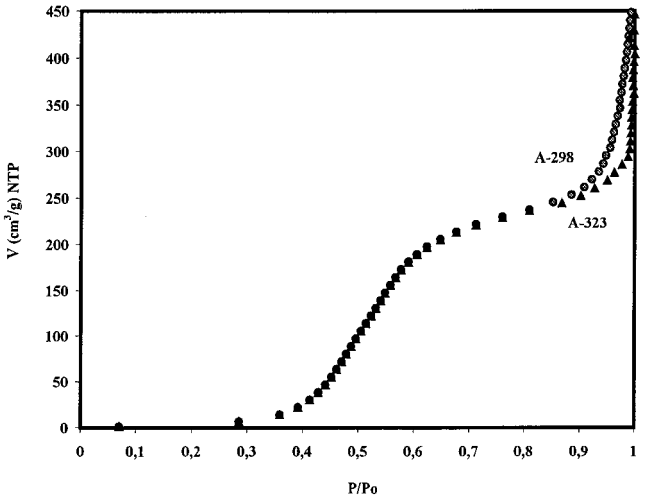

Figure 10. Water isotherms at 298 and 323 K on sample A.

P/P_0 0.8−1. Hence, the most important factor for water adsorption in the mesopores is the wetting of the mesopore walls, i.e., the hydrophilicity. So, if these walls have a predominantly hydrophobic (graphitic) character, they remain unfilled under the experimental conditions.

Finally, to establish a comparison between micropore and mesopore filling, water adsorption at different temperatures was carried out. Figure 10 shows isotherms obtained from water adsorption at 298 and 323 K in sample A. Both isotherms overlap over all the range of relative pressure up to 0.8; this temperature invariance is again in accord with the micropore filling mechanism discussed above. However, in the region of $P/P_0 > 0.8$, the water adsorption is pushed to higher relative pressures as the adsorption temperature is increased. This dependence on temperature is in agreement with the capillary condensation mechanism (see last equation). Hence, these results (Figures 9 and 10), provide further support for the conclusion that the water adsorption at $P/P_0 > 0.8$ is realized according to the capillary condensation mechanism.

4. Conclusions

It is shown that the shape of the water isotherm has a clear correlation with the pore size distribution. Thus, water isotherms display type V on essentially microporous ACs, while the presence of meso- and macroporosity gives an isotherm shape

that tends toward type III. Thus, water adsorption is a good technique to assess all ranges of pore size, at least semiquantitatively. The slope of the isotherm lineal tract (on the range $P/P_0 = 0.3-0.8$) is related to the micropore size distribution.

The presence of surface groups affects the isotherm in two ways; they control the relative pressure at the onset of adsorption in micropores and the filling of meso- and macropores by capillary condensation through their effect on the contact angle with liquid adsorptive prevailing at the pore wall. However, unless there is a pore-blocking effect, they do not influence the extent of volume filling of micropores, which takes place via a volume filling mechanism. The density of the adsorbed phase in micropores is close to that of ice and probably close to the liquid value in meso- and macropores.

Micropore filling is not complete until a P/P_0 of about 0.82, when capillary condensation begins in samples with relatively low surface polarity. Condensation in macropores can be observed with this adsorptive, but only at relative pressures greater than 0.95. This is contrast to the limitation in pore size that can be assessed by the conventional adsorptive, nitrogen.

Acknowledgment. J. Alcañiz would like to thank The Leverhulme Trust for the award of a visiting fellowship to the Department of Materials at the University of Leeds, U.K., where part of this collaborative study was carried out. We also wish to thank Project MEC-CICYT (Proyect No. PB98-0983).

References and Notes

(1) Bansal, R. Ch.; Donnet, J.; Stoeckli, F. *Active Carbon*; Marcel Dekker: New York, 1988.
(2) Lowell, S.; Shields, J. E. *Powder, Surface Area and Porosity*, 3rd ed.; Chapman and Hall: Bristol, 1991.,
(3) Jankowska, H.; Swiatkowski, A.; Choma, J. In *Active Carbon*; Kemp, T. J., Ed.; Ellis Horwood: Chischester, 1991.
(4) Suzuki, M.; Doi, H. *Carbon* **1982**, *20*, 441.
(5) Barton, S. S.; Koresh, J. E. *Carbon* **1984**, *22*, 481.
(6) O'Koye, I. P.; Benham, M.; Thomas, K. M. *Langmuir* **1997**, *13*, 4054.
(7) Gregg, S. J.; Sing, S. K. W. *Adsorption, Surface Area and Porosity*, 2nd ed.; Academic Press: London, 1982.
(8) Dubinin, M. M. *Carbon* **1980**, *18*, 355.
(9) Walker, P. L. Jnr.; Janov, J. *J. Colloid Interface Sci* **1968**, *28*, 499.
(10) Barton, S. S.; Koresh, J. E. *J. Chem. Soc., Faraday Trans. 1* **1983**, *79*, 1147, 1157, 1165.
(11) Kaneko, K.; Inouke, K. *Carbon* **1986**, *8*, 772.
(12) Carrott, P. J. M.; Kenny, M. B.; Roberts, R. A.; Sing, K. S. W.; Theocharis, C. In *Characterisation of Porous solids II*; Rodriguez-Reinoso, F., Rouquerol, J., Sing, K. S. W., Unger, K. K, Eds.; Elsevier: Amsterdam, 1991; p 685.
(13) Rodriguez-Reinoso, F.; Molina-Sabio, M.; Muñecas, M. A. *J. Phys. Chem.* **1992**, *96*, 2707.
(14) Bradley, R. H.; Rand, B. *J. Colloid Interface Sci.* **1995**, *169*, 168.
(15) Vartapetyan, R. Sh.; Voloshchuk, A. M. *Russ. Chem. Rev.* **1995**, *64*, 985.
(16) McBain, J. W.; Porter, J. L.; Sessions, R. F. *J. Am. Chem. Soc.* **1933**, *55* (5), 2294.
(17) Juhola, A. J.; Wiig, E. O. *J. Am. Chem. Soc.* **1949**, *71*, 2069.
(18) McDermott, H. L.; Arnell, J. C. *J. Phys. Chem.* **1954**, *58*, 492.
(19) Kadlec, O.; Varhanikova, A.; Zukal, A. *Carbon* **1970**, *8*, 321.
(20) Bansal, R. C.; Dhami, T. L.; Parkash, S. *Carbon* **1978**, *16*, 389.
(21) Mahle, J. J.; Friday, D. K. *Carbon* **1989**, *27*, 835.
(22) Juhola, A. J. *Kem. - Kemi* **1977**, *4*, 543.
(23) Sutherland, J. W. In *Porous Carbon Solid*; Bond, R. L., Ed.; Academic Press: London, 1970; pp 1−64.
(24) Pierce, C.; Smith, R. N. *J. Phys. Chem.* **1950**, *54*, 784.
(25) Dubinin, M. M.; Zaverina, E. D.; Serpinsky, V. V. *J. Chem. Soc.* **1955**, 1760.
(26) Dubinin, M. M.; Sherpinsky, V. V. *Carbon* **1981**, *19*, 402.
(27) Müller, E. A.; Gubbins, K. E. *Carbon* **1998**, *36*, 1433.
(28) McCallum, C. L.; Bandosz, T. J.; McGrother, S. C.; Müller, E. A.; Gubbins, K. E. *Langmuir* **1999**, *15*, 533.
(29) Iiyama, T.; Nishikawa, K.; Suzuki, T.; Otowa, T.; Hijiriyama, M.; Nojima, Y.; Kaneko, K. *J. Phys. Chem. B* **1997**, *101*, 3037.
(30) Iiyama, T.; Nishikawa, K.; Suzuki, T.; Kaneko, K. *Chem. Phys. Lett.* **1997**, *274*, 152.
(31) Iiyama, T.; Nishikawa, K.; Otowa, T.; Suzuki, T.; Kaneko, K. In *Characterisation of Porous Solids IV*.; McEnaney, B., May, T. J., Rouquerol, J., Rodriguez-Reinoso, F., Sing, K. S. W., Unger, K. K. K., Eds.; Royal Society of Chemistry: London, 1998; 41.
(32) Iiyama, T.; Ruike, M.; Suzuki, T.; Kaneko, K. In *Characterisation of Porous Solids V*.; Unger, K. K. K., Kreysa, G., Baselt, J. P., Eds.; Elsevier Science: Amsterdan, 2000; p 355.
(33) Kaneko, K. K. *Carbon* **2000**, *38*, 287.
(34) Salame, I. I.; Bandosz, T. *J. Colloid Interface Sci.* **1999**, *210*, 367.
(35) Salame, I. I.; Bandosz, T. *Langmuir* **1999**, *15*, 587.
(36) Kaneko, K.; Katori, T.; Shimizu, K.; Shindo, N.; Maeda, T. *J. Chem. Soc., Faraday Trans.* **1992**, *88*, 1305.
(37) Kaneko, Y.; Ohbu, K.; Uekawa, N.; Fujie, K.; Kaneko, K. *Langmuir* **1995**, *11*, 708.
(38) Stoeckli, F.; Kraehenbuehl, K.; Morel, D. *Carbon* **1983**, *21*, 589.
(39) Carrasco-Marín, F.; Mueden, A.; Centeno, T. A.; Stoeckli, F.; Moreno-Castilla, C. *J. Chem. Soc., Faraday Trans.* **1997**, *93*, 2211.
(40) Wintgens, D.; Lavanchy, A.; Stoceckli, F. *Ads. Sci. Technol.* **1999**, *17*, 761.
(41) Stoeckli, F.; Lavanchy, A. *Carbon* **2000**, *38*, 475.
(42) López-Ramón, M. V.; Stoeckli, F.; Moreno-Castilla, C.; Carrasco-Marín, F. *Carbon* **2000**, *38*, 825.
(43) Hanzawa, Y.; Kaneko, K. *Langmuir* **1997**, *13*, 5802.
(44) Kaneko, K.; Hanzawa, Y.; Iiyama, T.; Kanda, T.; Suzuki, T. *Adsorption* **1999**, *5*, 7.
(45) Alcañiz-Monge, J.; Linares-Solano, A.; Rand, B. *J. Phy. Chem. B* **2000**, submitted for publication.
(46) Alcañiz-Monge, J.; Cazorla-Amorós, D.; Linares-Solano, A. *Carbon* **1997**, *35*, 1665.
(47) Illán-Gómez, M. J.; García-García, A.; Salinas-Martínez de Lecea, C.; Linares-Solano, A. *Energy Fuels* **1996**, *10*, 1108.
(48) Cazorla-Amorós, D.; Ribes-Pérez, D.; Román-Martínez, M. C.; Linares-Solano, A. *Carbon* **1996**, *34*, 869.
(49) Román-Martínez, M. C.; Cazorla-Amorós, D.; Linares-Solano, A.; Salinas-Martínez de Lecea, C.; Atamny, F. *Carbon* **1996**, *34*, 719.
(50) Dubinin, M. M.; Raduskevich, L. V. *Proc. Acad. Sci. SSSR* **1947**, *55*, 331.
(51) Rodríguez-Reinoso, F.; Linares-Solano, A. In *Chemistry and Physics of Carbon*; Thorwer, H., Ed.; Marcell Dekker Inc: New York, 1988; pp 2−146.
(52) Naono, H.; Hakuman, M. *J. Colloid Interface. Sci.* **1991**, *145*, 405.
(53) Sing, K. S. W.; Everett, D. H.; Haul, R. A. W.; Moscou, L.; Pierotti, R. A.; Rouquerol, J.; Siemieniewska, T. *Pure Appl. Chem.* **1985**, *57*, 603.
(54) Lodewyckx, P.; Vansant, E. F. *Carbon* **1999**, *37*, 1647.
(55) Tsunoda, R. *J. Coll. Int. Sci.* **1990**, *137*, 563.
(56) Carrott, P. J. M. *Carbon* **1991**, *29*, 507.
(57) Freeman, J. J.; Tomlinson, J. B.; Sing, K. S. W.; Theocharis, C. R. *Carbon* **1993**, *31*, 865.
(58) Lentz, H.; Zhou, Y. In *Characterisation of Porous solids II*; Rodriguez-Reinoso, F., Rouquerol, J., Sing, K. S. W., Unger, K. K, Eds.; Elsevier: Amsterdam, 1991; p 499.
(59) Dubinin, M. M. *Chem. Rev.* **1960**, *60*, 235.
(60) Stoeckli, F.; Jakubov, T. S.; Lavanchy, A. *J. Chem. Soc., Faraday Trans.* **1994**, *90*, 783.
(61) Naono, H.; Shimoda, M.; Morita, N.; Hakuman, M.; Nakai, K.; Kondo, S. *Langmuir* **1997**, *13*, 1297.
(62) Hassan, N. M.; Ghosh, T. K.; Hines, A. L.; Loyalka, S. K. *Carbon* **1991**, *29*, 681.
(63) Do, D. D.; Do, H. D. *Carbon* **2000**, *38*, 767.
(64) Adamson, A. W. *Physical Chemistry of Surfaces*, 5th ed.; Wiley: New York, 1990; p 397.